C. R. Chimie 20 (2017) 475–483

Contents lists available at ScienceDirect

Comptes Rendus Chimie

www.sciencedirect.com

Full paper/Mémoire

Antimicrobial performance of nanostructured silica–titania sieves loaded with izohidrafural against microbial strains isolated from urinary tract infections

Mustafa Basim M. Al Tameemi [a], Raluca Stan [a, *], Viorel Prisacari [b], Georgeta Voicu [a], Marcela Popa [c], Mariana Carmen Chifiriuc [c], Cristina Ott [a], George Marton [a], Aurelia Meghea [a]

[a] *Faculty of Applied Chemistry and Material Science, Politehnica University of Bucharest, Polizu Street No. 1-7, 011061 Bucharest, Romania*

[b] *"Nicolae Testemitanu" State University of Medicine and Pharmacy, 165, Stefan cel Mare Boulvard, Chisinau, MD 2001, Republic of Moldova*

[c] *Faculty of Biology, Microbiology Immunology Department, University of Bucharest, Aleea Portocalelor No. 1-3, 060101 Bucharest, Romania*

ARTICLE INFO

Article history:
Received 15 June 2016
Accepted 19 September 2016
Available online 22 October 2016

PubChem CID for the essential compounds used in this article:
TEOS (PubChem CID: 6517)
CTAB (PubChem CID: 5974)
Titanium (PubChem CID: 23963)
Sulfuric acid (PubChem CID: 1118)
Ammonium fluoride (PubChem CID: 25516)
Nitrofurantoin (PubChem CID: 6604200)

Keywords:
Silica–titania sieves
Antimicrobial activity
Izohidrafural
Urinary tract infections
Synergistic effect

ABSTRACT

This study aimed to examine the efficiency of novel bioactive nanostructures represented by silica–titania sieves used as carriers for a new antibacterial agent izohidrafural against bacterial strains isolated from nosocomial urinary tract infections, by using biological quantitative assays. Several release trials have been established and compared with **MCM-41** in parallel experiments to achieve the optimum release profile. The obtained systems showed that silica–titania sieves loaded with izohidrafural proved to be the most active material against *Klebsiella pneumoniae* (average minimal inhibitory concentration [MIC] 40.62 μg/mL), desaminase-positive strains (average MIC 2.925 μg/mL), and *Proteus mirabilis* (average MIC 9.37 μg/mL), the last being reported with the highest growth rate in the urinary tract catheters. In contrast, the nonloaded silica–titanium sieves exhibited the highest antimicrobial activity against the Gram-positive cocci. Izohidrafural exhibited the highest antimicrobial efficiency, superior to the common drug nitrofurantoin against most *Escherichia coli* strains, with average MIC of 4.68 μg/mL.

1. Introduction

The infectious diseases are considered as one of the most important health issues around the world because of many challenges posed by the emergency of antibiotic resistant strains [1] and the inability of many classes of antibiotics to reach the intracellular bacterial strains [2,3]. Nosocomial infections afflict one of 10 patients admitted to the hospital. These types of infections might be caused by Gram-negative bacteria, Gram-positive bacteria, and other types of microorganisms [4]. Urinary tract infections (UTIs) are considered as one of the most widespread nosocomial

* Corresponding author.
E-mail addresses: rl_stan2000@yahoo.com, raluca.stan@chimie.upb.ro (R. Stan).

http://dx.doi.org/10.1016/j.crci.2016.09.007
1631-0748/

infections [5], they are representing also one of the most common pathology encountered in community with a prevalence varying from 0.7% in community-acquired infections to 24% among health care–associated infections, and these numbers vary depending on the geographical area [6]. The most prevalent microorganism involved in the etiology of UTI is *Escherichia coli*, followed by *Klebsiella pneumoniae*, *Proteus* sp., *Enterobacter* sp., *Pseudomonas* sp., *Enterococcus* sp., and *Staphylococcus* sp. [7,8].

In the past few years, an increasing trend in the antibiotic resistance in these isolates has been observed. Resistance to most available antibiotics in hospital-acquired UTIs is currently more than 20%, and the increasing isolation rates of multidrug, extended-drug, and pan-drug–resistant bacterial strains are urging the development of novel antimicrobial agents and strategies [9]. Retention of the antibiotic in the therapeutic level without increasing the drug dosages represents the point of challenge in many research works while seeking to specific drug administration in the living body. Nowadays, with the evolution of nanotechnology, high performance of drug delivery can be achieved through controlling the release profile with certain nanoscaled drug delivery systems. The suitable systems for the antibiotic agents can be achieved by using antimicrobial nanoparticles or nanosized drug carriers for delivering these antibiotics [1].

Various types of nanomaterials have been reported as vehicles for antibiotic administration such as carbon nanotubes, gold nanoparticles, and nanostructured silica materials [10,11]. Mesoporous silica materials present a good biocompatibility, and because of the presence of free silanol active groups within their porous structure are able to successfully encapsulate and slow release various types of biologically active compounds and thus antimicrobial agents [10,12,13]. Furthermore, the well-designed mesoporous silica possesses high surface area allowing to accommodate large amounts of antibiotics, tuned pore sizes with narrow distribution determining well-controlled release profile [14,15]. For example, silica xerogel has been reported to be a carrier for gentamicin to increase the intracellular penetration [16]. SBA-15 was also investigated as an antibiotic delivery system for tetracycline [17], and amino-modified SBA-15 was investigated to deliver clarithromycin [18]. Mesoporous silica sieves such as **MCM-41**-type nanocomposites have been widely investigated for delivery of antibiotics. Some **MCM-41**-type composites modified with aluminum used as delivery systems for amikacin, an aminoglycoside antibiotic, were reported to improve retention of the drug with slower release kinetics [10]. These materials were also reported as delivery systems for other kinds of antibiotics such as vancomycin [11] and nitrofurazone [13].

The combination between silica and biocompatible metals or derivatives may be extended from aluminum to other metals with improved biological activity, for example, gold [19] or titanium dioxide. The presence of titanium dioxide into mesoporous silica composites enhances the specific surface, modifies the activity of the silica surface, and provides photocatalytic activity, thus conferring a good disinfectant activity [20].

In this study, we used a new encapsulation support, nanostructured silica-titania sieves which combines the advantages of the silica nanomaterials in terms of microporosity or nanoporosity [21] with their ability to encapsulate antibiotics and prolonged release [18,22]. These advantages have been employed along with titanium dioxide properties in the anatase form, known for its photocatalytic effect and antibacterial activity [23]. By loading suitable antimicrobial into these sieves, we may provide a bioactive cover for the urinary tract catheters. Stickler [24] confirmed that catheters provide ideal conditions for the growth of many bacterial species colonized as biofilm, *Proteus mirabilis* being the most abundant among them.

The recently reported silica–titania sieves were used for encapsulation of a new drug, izohidrafural (izonicotinoilhidrazone aldehyde 5-nitro-2-furan) a stable organic compound from the class of nitrofurane-type antibacterial agents. Izohidrafural (Fig. 1c) has been synthesized from 5-nitrofurfural and isoniazid, characterized, and its biological properties investigated by Prisacari co-authors [25,26]. Izohidrafural proved to be by two to four times more active toward both Gram-negative and Gram-positive types of bacteria and exhibits nine times less toxicity than the parent compound nitrofurazone (Fig. 1a) against a large number of microorganisms responsible for nosocomial infections and longer-term stability [27]. However, no data were provided for comparison of the antimicrobial activity of izohidrafural with the commonly used nitrofurantoin (Fig. 1b) employed for decades as an alternative to sulfamethoxazole and fluoroquinolones for the first-line treatment of uncomplicated UTIs, preserving a high rate of susceptibility among uropathogenic strains and having a favorable adverse-effect profile [28,29].

To establish the influence of titanium dioxide on the silica matrix as a carrier for nitrofurane-derived antibacterials, a parallel encapsulation/release experiment was conducted using **MCM-41** and the same antimicrobial agent, izohidrafural. The secondary goal of this study attempts to elucidate the ability of **MCM-41** to encapsulate and to provide prolonged release of izohidrafural, being reported that the parent compound, nitrofurazone, failed the loading experiment in **MCM-41** [13]. The biological

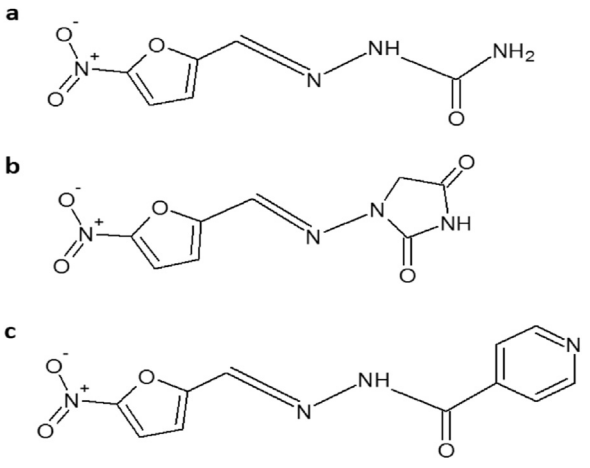

Fig. 1. Chemical structures of (a) nitrofurazone, (b) nitrofurantoin, and (c) izohidrafural.

activity tests were conducted for both free and encapsulated izohidrafural having as reference nitrofurantoin on 15 strains of Gram-negative and Gram-positive strains isolated from nosocomial UTIs.

2. Materials and methods

2.1. Materials

Chemicals, tetraethyl orthosilicate (TEOS), metallic titanium, cetyltrimethylammonium bromide (CTAB), concentrated sulfuric acid, ammonium aqueous solution, ammonium fluoride, and ethanol were obtained from Sigma–Aldrich and used as received. Izohidrafural (**Izo**) was supplied by "Nicolae Testemitanu" State Medical and Pharmacy University, Chisinau, Republic of Moldova, and used as received. Nitrofurantoin (*N*-(5-nitro-2-furfurylidene)-1-aminohydantoin; **NF**) was obtained from Sigma–Aldrich and used as received. All the experiments were conducted using ultrapure water type 2 (~15 MΩ) obtained from a Millipore Elix5 device.

2.2. Synthesis of *MCM-41*

MCM-41 was prepared according to a previously reported procedure [30] by mixing a solution of 2 mL (9 mmol) of TEOS in 34 mL of ethanol with a solution of 0.5 g (1.4 mmol) of CTAB in 96 mL of water, followed by dropwise addition of 10 mL (134 mmol) of 25% ammonia aqueous solution. The reaction mixture was stirred for 3 h (400 rpm) and then left overnight. The resulted silica gel material was filtered, dried at room temperature, and calcinated for 3 h at 550 °C with a heating rate 5°/min.

2.3. Synthesis of silica–titania sieves

Silica–titania sieves (**Si-Ti-Sv**) were prepared following our previously reported procedure [21]. To a solution of silica precursor consisting of 7.6 mL (34 mmol) of TEOS and 11 mL of methanol, a surfactant solution of 0.5 g (1.4 mmol) of CTAB dissolved in 11 mL of methanol and 7 mL of water was added followed by the addition 0.3 g (8 mmol) of ammonium fluoride as a catalyst and 2.5 mL of 25% ammonium hydroxide solution to control the pH. Separately, a stock solution of titanium dioxide precursor was prepared by dissolving 5 g (104 mequiv) of metallic titanium powder in 50 mL (940 mmol) of concentrated sulfuric acid and stirred (400 rpm) at 100 °C for 3 h. The titanium dioxide precursor solution was prepared before the experiment by diluting 1.9 g of the stock solution (2 mequiv Ti) with 11 mL of methanol and 10 mL of water and subsequently added to the previous reaction mixture and stirred (400 rpm) at room temperature for 24 h. The resulted material was filtered, washed repeatedly with water and ethanol, left to dry at room temperature, and finally calcinated at 650 °C for 6 h with a heating rate 5°/min.

2.4. Characterizations

Fourier transform infrared (FT-IR) spectra were recorded using Thermo Nicolet 6700. Brunauer–Emmett–Teller (BET) analysis was carried out on a Micrometrics Gemini V2 model 2380. The adsorption isotherms were obtained by measuring the quantity of the adsorbed gas at a wide range of relative pressures with constant temperature (N_2, 77 K and pressure between 780 and 7.8 mmHg). Desorption isotherms were obtained by measuring the gas desorption rate at pressure reduction. UV–vis spectra were recorded on Thermo scientific evolution 220. The release experiments were performed using the pump and the UV detector of a High-performance liquid chromatography (HPLC) Agilent 1100 system.

2.5. Drug loading

The loading experiments were carried out by mixing 15 mg of the prepared nanostructured materials with **Izo** in 10 mL of water for 24 h. Three different ratios (12:1, 6:1, and 3:1) of carrier/drug were used to achieve the best encapsulation efficiency (Table 1). The loaded material was filtered and washed with 30 mL of water and finally dried at room temperature. The filtrate and the washing waters were collected to estimate the encapsulation efficiency.

2.6. Encapsulation efficiency

The encapsulation efficiency of **Izo** in the nanostructured materials was evaluated using the UV absorbance at λ_{max} = 362 nm for **Izo** according to the Lambert–Beer law. The concentration of free drug in the combined filtrate and washings was analyzed using the calibration curve in the concentration range of the calibrations 0.04–8 mg/L **Izo**, with a correlation coefficient 0.9985. The encapsulation efficiency was calculated using the following formula:

$$EE\% = \frac{C_{Izoinitial} - C_{izofree}}{C_{Izoinitial}} \times 100$$

The absorbed drug/carriers ratios are presented in Table 2.

2.7. Drug release

The drug release experiments were performed using the procedure previously reported [31] by placing the loaded nanomaterials in the release medium consisting of 500 mL of water stirred at 400 rpm and by continuously collecting aliquots of the release medium using the HPLC pump

Table 1
The mixed ratios of the drug (**Izo**) with both nanostructured carrier materials, **MCM-41** and **Si-Ti-Sv**.

Loaded material	**MCM-41-Izo1**	**MCM-41-Izo2**	**MCM-41-Izo3**	**Si-Ti-Sv-Izo1**	**Si-Ti-Sv-Izo2**	**Si-Ti-Sv-Izo3**
Carrier/drug ratio	0.083	0.166	0.333	0.083	0.166	0.333

Table 2
The loaded ratios of the drug (**Izo**) with both nanostructured carrier materials, **MCM-41** and **Si-Ti-Sv**.

Loaded material	MCM-41-Izo1	MCM-41-Izo2	MCM-41-Izo3	Si-Ti-Sv-Izo1	Si-Ti-Sv-Izo2	Si-Ti-Sv-Izo3
Carrier/absorbed drug ratio	0.060	0.146	0.306	0.061	0.136	0.296

equipped with UV detector. Looping system has been achieved continuously by placing the inlet and the outlet of this system in the same release medium. The amount of released drug was estimated spectrophotometrically at $\lambda_{max} = 362$ nm using a calibration curve in the concentration range of 0.04–8 mg/L with the correlation coefficient of 0.9985.

2.8. Antimicrobial activity assays

The antimicrobial activity spectrum and minimal inhibitory concentration (MIC) of the **Si-Ti-Sv**, **Si-Ti-Sv-Izo3**, **Izo**, and **NF** was assayed on Gram-negative and Gram-positive strains isolated from UTIs (*E. coli—EC* 2622, *E. coli* 2739, *E. coli* 2645, *E. coli* 2749, *E. coli* 2646, *E. coli* 2732, *E. coli* 2598, *K. pneumoniae* 2727, *K. pneumoniae—Kp* 2633, *K. pneumoniae* 2770, *Morganella morganii* 2651, *P. mirabilis—Pm* 2648, *Enterococcus feacalis—EF* 2788, *Enterococcus faecalis* 2842) using *E. coli* ATCC 8739 as a reference strain. Microbial suspensions of 1.5×10^8 CFU/mL (0.5 McFarland density) obtained from 15 to 18 h bacterial cultures developed on solid media were used in our experiments. The compounds were solubilized in Dimethyl sulfoxide (DMSO) and the starting stock solution was of 1.2 mg/mL concentration.

The *qualitative assay of the antimicrobial activity* was performed on the Mueller–Hinton Agar medium by an adapted disc-diffusion method as previously reported [32]. The quantitative assay of the antimicrobial activity was performed by the liquid medium microdilution method in 96-multiwell plates to establish the MIC. For this purpose, 10 serial twofold dilutions of the compound solutions (starting from 600 μg/mL) were performed in a 200 μL volume of broth, and each well was seeded with 50 μL microbial inoculum. Culture positive controls (wells containing culture medium seeded with the microbial inoculum) were used. The influence of the DMSO solvent was also quantified in a series of wells containing DMSO, diluted according to the dilution scheme used for the complexes. The plates were incubated for 24 h at 37 °C, and MIC values were considered as the lowest concentration of the tested compound that inhibited the growth of the microbial overnight cultures, as compared with the positive control, revealed by a decreased value of absorbance at 600 nm measured in triplicate [33–36].

3. Results and discussion

3.1. Encapsulation of the drug

Izo has been loaded into the **Si-Ti-Sv** and **MCM-41** by mixing these materials separately with the drug in an aqueous solution. The presence of **Izo** into both silica materials has been determined using FT-IR by identifying characteristic absorption vibrations of the drug in the loaded material (Fig. 2). The unloaded sieves, **Si-Ti-Sv**, present a stretching broad band at 1053.77 cm^{-1} assigned to asymmetric Si-O vibration (Fig. 2A-a). In addition, a small band at 802.41 cm^{-1} is related to the symmetric stretching of Si-O bonds [38]. The antimicrobial drug **Izo** presents several characteristic absorptions as follows: 3389 cm^{-1}(υ_{N-H}, secondary amide); 2967.51 and 2930.40 cm^{-1} ($\upsilon_{=C-H}$, substituted furane); 1682.63 cm^{-1} ($\upsilon_{C=O}$ and secondary amide); and 1520.06 and 1348.73 cm^{-1} ($\upsilon_{N-O,}$ nitro group), which are in good agreement with the reported data [25]. The last three absorptions were used as “markers” for the encapsulated drug (Fig. 2A-b, c).

Shifting for the characteristic FT-IR bands of the encapsulated drug was observed and rationalized as the influence of hydrogen bonding with hydroxyl groups exhibited on the surface of a nanostructured hybrid material, more pronounced for **Si-Ti-Sv** (Fig. 2A-c) than **MCM-41** (Fig. 2B-c), which is in good agreement with the increased density of OH groups brought by anatase [37].

Encapsulation efficiency of **Izo** into the nanostructured silica materials was influenced by the initial ratio of drug/carrier and increased with the amount of drug from 73% for 1:12 ratio up to ~90% for 1:3 ratio, respectively (Fig. 3). Comparable efficiencies were observed for the two materials with a slight superiority of **MCM-41**—92% for 1:3 ratio—as compared with 89% for **Si-Ti-Sv** for the same loading ratio. Because of the low water solubility of **Izo**, we presume that diffusion of the drug into the pores is more efficient for **MCM-41**, which presents a higher BET surface area (1716.15 m^2/g) and larger pore size diameter (7.7 nm). On the contrary, the absorption on **Si-Ti-Sv** occurs mainly on the surface because of smaller size of pores (4.5 nm) but is strongly influenced by the higher density of OH groups on the surface brought by anatase, even if the BET surface area is less than half (613.60 m^2/g). This assumption is in good agreement with the release curves in the drug release experiments (Fig. 4).

3.2. Drug release

The release study has been done first to the samples which has the lowest drug ratio of 0.083 for both materials **Si-Ti-Sv-Izo1** and **MCM-41-Izo1** (Fig. 4). The choice of the low **Izo**/carriers ratio was preferred in the attempt to achieve the zero-order kinetic (no dependency on the solubility) according to the poor solubility of the drug in water. **MCM-41-Izo1** demonstrated the highest release ratio up to more than 90% of the **Izo** after more than 6 h. The release percentage of the drug of 77% from **MCM-41-Izo1** in the first 50 min shows a weak affinity of **Izo** for this type of material similarly with reported data for the parent compound nitrofurazone [13].

On the other hand, **Si-Ti-Sv-Izo1** release profile was significantly different, the cumulative release percentage was around 40% in the first 50 min and only 74% of the drug was released until about 6.5 h (Fig. 4b). The slow release from loaded silica–titanium sieves may be explained by a

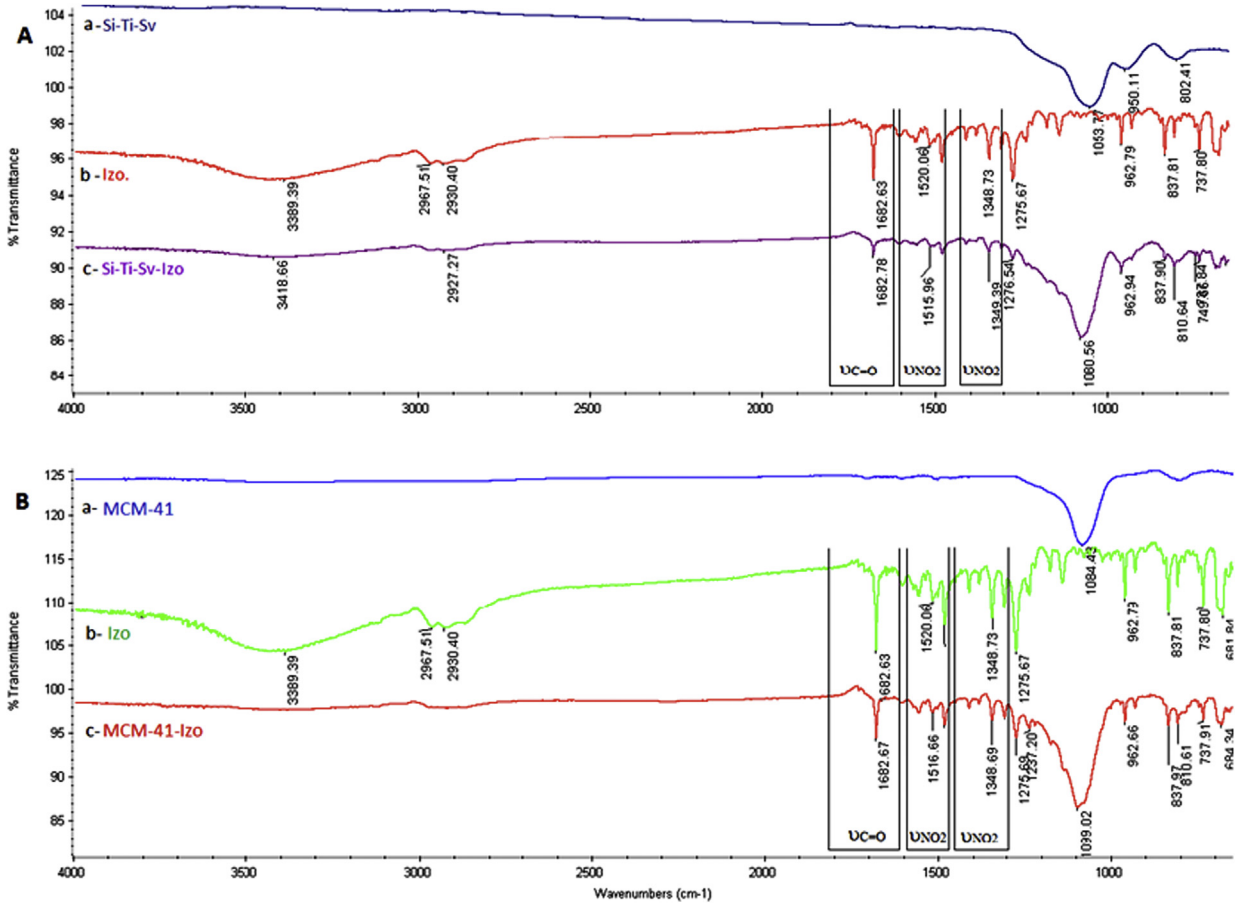

Fig. 2. FT-IR absorbance bands of A (a) **Si-Ti-Sv**, (b) **Izo**, and (c) **Si-Ti-Sv-Izo** and B (a) **MCM-41**, (b) **Izo**, and (c) **MCM-41-Izo**.

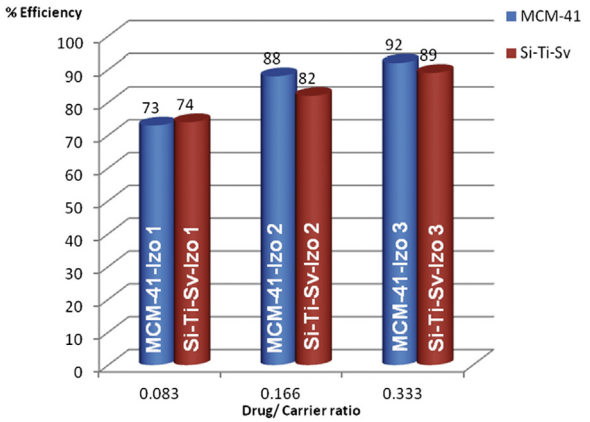

Fig. 3. Encapsulation efficiencies of **Izo** into the nanostructured silica materials.

better adsorption of the drug on the surface of a material because of a higher amount of free hydroxyl groups brought by titanium dioxide nanoparticles fixed on the surface of silica oxide, as revealed by reported Transmission Electron Microscopy (TEM) micrographs [21]. According to the literature data, the amount of −OH surface density of TiO_2 is almost double as compared to SiO_2, enabling an efficient hydrogen bonding with structural moieties of **Izo** [38].

For a better understanding of the encapsulation/release behavior of **Izo**, we have performed quantum mechanics calculations on this molecule using General Atomic and Molecular Electronic Structure System (GAMESS) [39] at M11/Karlsruhe valence triple zeta basis with a set of single polarization (KTZVP) level of theory. The minimized geometry, electron density, and Debye moment were calculated. The graphical representation of the calculus results on **Izo** is obtained with MacMolPlt [40] and Gabedit [41] and is presented in Fig. 5. The total electron density computed for the molecule of the drug **Izo** is colorized according to molecular electrostatic potential. The contour is at 0.04 au on an isodensity surface of 0.03 au (Hartrees/electronic charge), blue representing the most negative potential (approximately −0.03 au).

As it can be seen from the total electron density distribution depicted in Fig. 5, there are four sites around the nitro group, carbonyl, and nitrogen from pyridine moiety with increased electron density, creating good premises for hydrogen bonding with hydroxyl groups existent on the surface of nanostructured materials used for loading (e.g., **Si-Ti-Sv**), and this association is sustained by the shift observed for the characteristic FT-IR absorptions of the

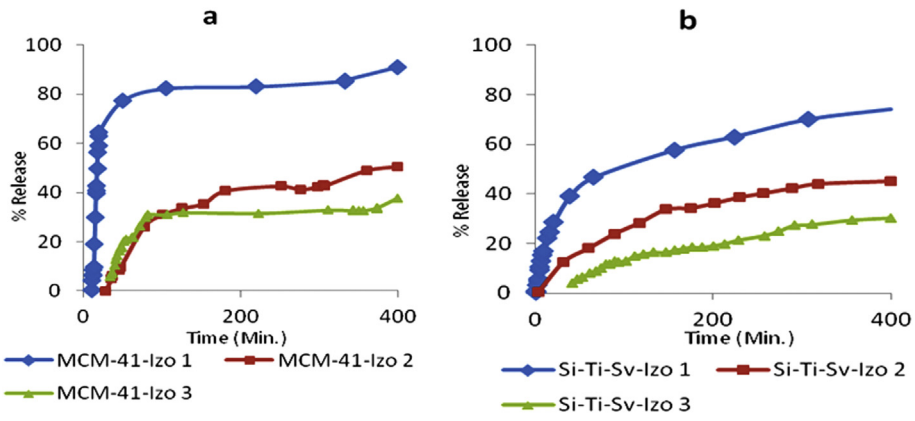

Fig. 4. Release profile of **Izo** from (a) **MCM-41-Izo1-Izo3** and (b) **Si-Ti-Sv-Izo1-Izo3**.

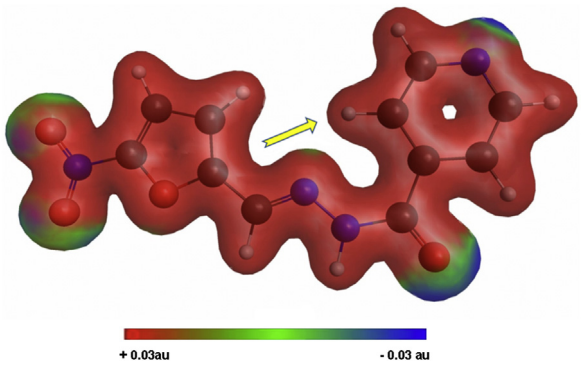

Fig. 5. Minimized geometry, electron density, and Debye moment orientation calculated for **Izo**.

encapsulated drug. On the other hand, the orientation of the calculated dipole moment along the molecular axis, represented by the displayed arrow in Fig. 5, favors the penetration of the molecule in polar cavities as, for example, those of mesoporous **MCM-41**.

3.3. Biological tests

The drug-loaded materials with the highest drug/carrier ratio were selected for biological tests to have a good comparison both with the biological activity of the carrier and the unloaded drug, respectively, taking into account the results obtained in the release experiments for the most concentrated samples. Only 30% of the drug was released after 6 h, leading to an absolute quantity of the drug almost double than for the lowest concentrated ones. The biological test performed on clinical strains recently isolated from UTI to comparatively evaluate the **Si-Ti-Sv**, **Si-Ti-Sv-Izo3**, **Izo**, and the common **NF** as a reference. In the same context, this test was performed to evaluate the antimicrobial activity of the novel hybrid material loaded or not with **Izo** against Gram-negative and Gram-positive bacterial strains isolated from UTIs in the hospital environment, exhibiting antibiotic resistance rates to the current antibiotics.

In the qualitative assay, we have quantified the growth inhibition zone diameters induced after the deposition of 10 μL of the DMSO stock solution (12 mg/mL concentration) over the microbial culture. The DMSO solvent used did not influence the antimicrobial activity of the tested compounds at the working concentrations. The test revealed that the free drug **Izo** proved to exhibit the largest antimicrobial spectrum and the highest activity similar to **NF** against the tested strains (Fig. 6).

The quantitative assay of the antimicrobial activity of the tested compounds revealed that the MIC values were different depending on the tested compounds and the microbial strains. The lowest MIC values obtained in the quantitative assay measurements are summarized in Fig. 7 for every type of microorganism and tested materials and antimicrobials. As depicted in Fig. 7, the reference drug, **NF**, exhibited MIC values ranging from 300 to 4.68 μg/mL against the *E. coli*, from 18.75 to 1.17 against *K. pneumoniae*, from 75 to 9.37 for desaminase-positive enterobacteria (*P. mirabilis* and *M. morganii*) and >600 μg/mL in case of *Enterococcus faecium* strains. The newly tested drug **Izo** exhibited a very good antimicrobial activity againstt the *E. coli* strains, superior to that of **NF**, with a low MIC value of 4.68 μg/mL for most tested strains except *E. coli* 8739. On the contrary, the **Izo** drug was less active against *K. pneumoniae* strains, exhibiting a high MIC value of 600 μg/mL and urease producer cells, with MIC values >600 μg/mL against *M. morganii* and 18.75 μg/mL against *P. mirabilis*. Similar to **NF**, **Izo** was inefficient against the *Enterococcus faecium* strains, with MIC values >600 μg/mL.

The unloaded carrier, **Si-Ti-Sv** exhibited intermediate efficacy, higher than **NF** but lower than **Izo** against the *E. coli* strains, with MIC values ranging from 75 to 9.37 μg/mL and a moderate activity against *K. pneumoniae* strains with MIC values of 75–150 μg/mL. The activity of **Si-Ti-Sv** against the desaminase-positive enterobacteria was variable, being very good against *M. morganii* (MIC value of 2.34 μg/mL) and moderate toward *P. mirabilis* (MIC value of 150 μg/mL). **Si-Ti-Sv** exhibited very good activity against the Gram-positive cocci, with MIC values of 1.17 and 18.75 μg/mL, respectively. Finallyy, the drug-loaded sieves, **Si-Ti-Sv-Izo3** exhibited activity superior to **NF** and **Si-Ti-Sv**, comparative to unloaded drug, **Izo** against the *E. coli* strains, with MIC values of 4.68–18.75 μg/mL. **Si-Ti-Sv-Izo3** proved to be the most active against the *K. pneumoniae* strains, with the lowest MIC values ranging between 37.5 and 9.37 μg/mL

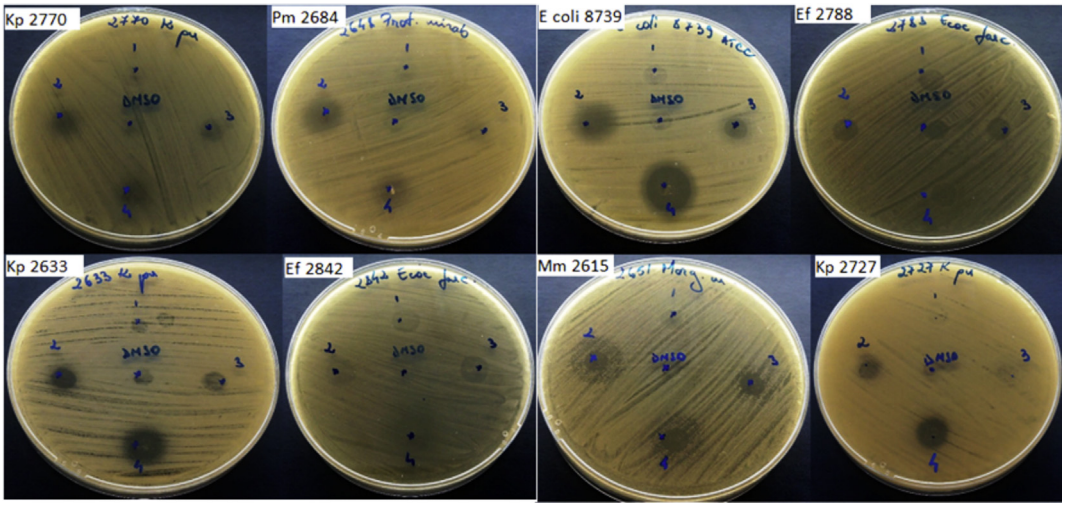

Fig. 6. Qualitative assay to determine growth inhibition zone diameters for tested microbial strains: (1) **Si-Ti-Sv**; (2) **Izo**; (3) **Si-Ti-Sv-Izo3**; and (4) **NF**.

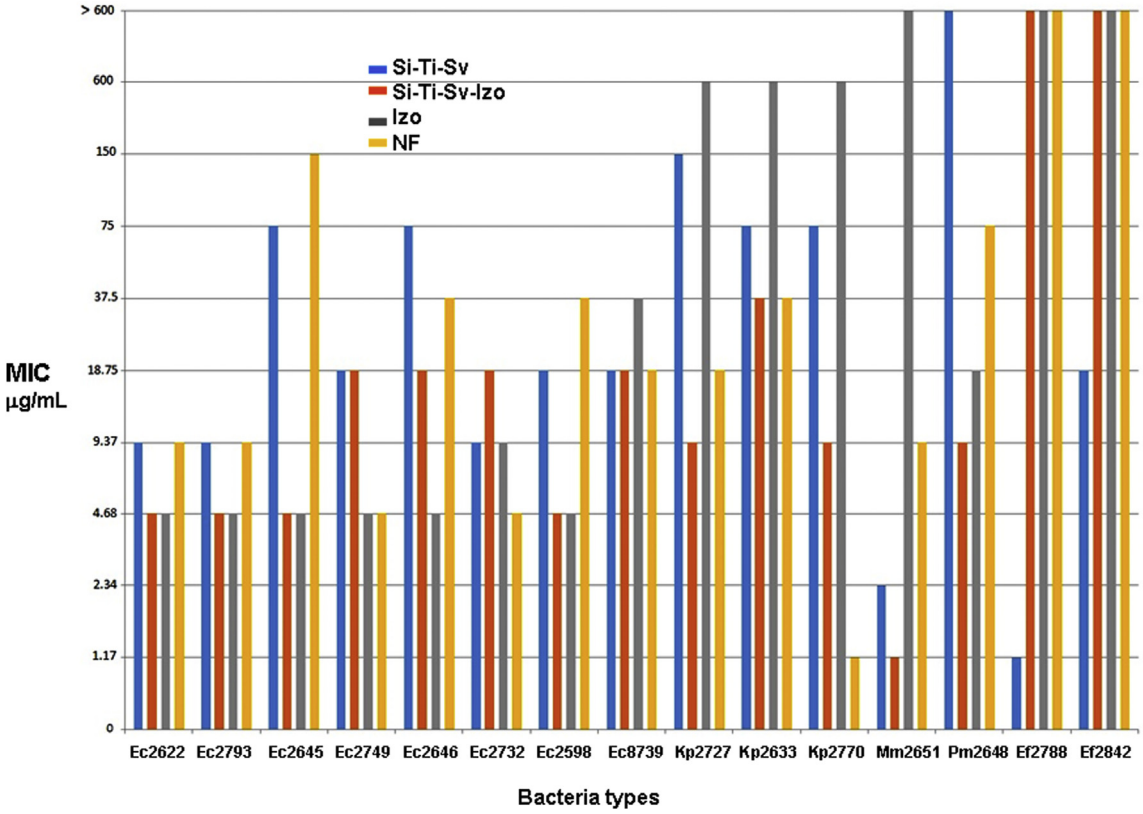

Fig. 7. Comparative results for the biological activity of **Si-Ti-Sv**, **Si-Ti-Sv-Izo3**, **Izo**, and **NF** against microorganisms involved in UTIs.

and against the desaminase-positive strains, with MIC values of 4.68–1.17 µg/mL. In return, this material proved to be inefficient against the Gram-positive bacterial strains, the MIC values being >600 µg/mL. In the particular case of *P. mirabilis*, the **Izo**-loaded sieves, **Si-Ti-Sv-Izo3**, present the lowest MIC value (9.37 µg/mL) as compared with the free tested drugs, **NF** and **Izo**, providing a promising material for antimicrobial external protection of catheters.

The results of antibacterial tests presented in Fig. 7 revealed that in some experiments involving Gram-negative bacterial strains, such as Kp 2727, Kp 2770, Mm 2615, and Pm 2648, a synergistic effect has been observed. For example, unloaded sieves and pure **Izo** exhibited MIC values superior than those determined for the reference drug **NF**. On the contrary, the lowest value for MIC determined for Kp 2727, of 9.37 µg/mL, was obtained for loaded sieves (**Si-Ti-**

Sv-Izo3) which proved to be twice more active than **NF**, 16× and 64× superior to the unloaded hybrid material and **Izo**, respectively (Fig. 7). The same effect with different ratios between the corresponding determined values of MIC was observed for the other Gram-negative strains, such as Kp 2770, Mm 2651, and Pm 2648. This enhancement of the biological activity was not observed for the tested *E. coli* strains, the optimum MIC values for both loaded sieves and free **Izo** (e.g., EC 2622, EC 2793, EC 2645, and EC 2598), being the same although in some cases the unloaded sieves proved to be more active than the reference drug **NF**.

To explain the antibacterial performance of the tested materials, the unloaded and **Izo**-loaded hybrid nanomaterial, **Si-Ti-Sv**, we revised the reported mechanisms of action for the class of nitrofurane-derived antimicrobials and reported data on titanium dioxide [23,42]. Nitrofurane-derived antimicrobials act by inhibiting bacterial enzymes involved in DNA and RNA synthesis, carbohydrate metabolism, and other metabolic enzyme proteins, and no explanation regarding the influence of titanium dioxide on this type of mechanisms was readily available.

The synergistic effect might occur because titanium dioxide, in the form of anatase, contained in the hybrid **Si-Ti-Sv**, has photocatalytic properties and thus has the ability of creating reactive oxygen species such as superoxide ($O_2^{\bullet -}$), hydrogen peroxide (H_2O_2), hydroxyl radicals ($HO^{\bullet}$), and hydroperoxyl radicals ($HOO^{\bullet}$) that are harmful to cells [23]. On the other hand, the increased activity of **Izo** as compared to **NF** may be explained by the presence in the molecular structure of the drug of the isoniazid moiety, a potent antibacterial by itself. The reported mechanism for the biological activity of isoniazid states that in the presence of an oxidizing enzyme, KatG, the molecule is transformed into radical species such as acyl, acylperoxo, and pyridyl radicals [43]. Therefore, we may presume that titanium dioxide plays a role in activating **Izo**, thus producing a synergistic effect by generating a higher number of very reactive free radicals. The activity of the hybrid sieves on Gram-positive *cocci*, for example, EF 2788 and EF 2842, may be explained by the difference in the morphology of the cellular wall of this type of bacteria as compared to Gram-negative strains, which facilitates the penetration of reactive oxygen species generated by titanium dioxide [23].

4. Conclusions

In this article, we have investigated the antibacterial performance of a novel nanostructured hybrid material, based on silica–titania used for encapsulating and drug release experiments for a recently developed antibacterial drug from nitrofurane family, izohidrafural. The new hybrid material proved similar ability to encapsulate the tested drug as **MCM-41** but an improved release profile because of enhanced affinity of the hybrid sieves' surface for the bioactive molecules. The antimicrobial activity of izohidrafural-loaded hybrid sieves was evaluated against Gram-negative and Gram-positive strains isolated from UTIs in the hospital environment, exhibiting antibiotic resistance rates to the current antibiotics, using quantitative assay. For the tested Gram-positive *cocci* involved in UTIs, unloaded hybrid sieves proved to be the only active antibacterial agent with an average MIC value of 9.96 μg/mL, probably because of the presence of titanium dioxide. The novel carrier has significantly improved the antibacterial activity of the encapsulated drug for a series of tested Gram-negative bacteria, including *P. mirabilis*, a urease-producing bacteria responsible for crystalline biofilms in catheters, lowering the necessary concentrations up to two orders of magnitude because of a synergistic effect.

References

[1] A. Huh, Y.G. Kwon, J. Control. Release 156 (2011) 128–145, http://dx.doi.org/10.1016/j.jconrel.2011.07.002.
[2] A. Vazquez-Torres, J. Jones-Carson, A. Baumler, S. Falkow, R. Valdivia, W. Brown, M. Le, R. Berggren, W. Parks, F. Fang, Nature 401 (1999) 804–808, http://dx.doi.org/10.1038/44593.
[3] M. Seleem, N. Jain, A. Ranjan, J. Riffle, N. Sriranganathan, FEMS Microbiol. Lett. 294 (2009) 24–31, http://dx.doi.org/10.1111/j.1574-6968.2009.01530.x.
[4] K. Inweregbu, J. Dave, A. Pittard, Contin. Educ. Anaesth. Crit. Care Pain 5 (2005) 14–17, http://dx.doi.org/10.1093/bjaceaccp/mki006.
[5] A. Peleg, C. Hooper, N. Engl. J. Med. 362 (2010) 1804–1813, http://dx.doi.org/10.1056/NEJMra0904124.
[6] Z. Tandogdu, F.M. Wagenlehner, Curr. Opin. Infect. Dis. 29 (2016) 73–79, http://dx.doi.org/10.1097/QCO.0000000000000228.
[7] D.J. Farrell, I. Morrissey, D. Rubeis, M. Robbins, D. Felmingham, J. Infect. 46 (2003) 94–100, http://dx.doi.org/10.1053/jinf.2002.1091.
[8] S.R. Mirsoleymani, M. Salimi, M. Shareghi, M. Ranjbar, M. Mehtarpoor, Int. J. Pediatr. 2014 (2014) 6, 126142, http://dx.doi.org/10.1155/2014/126142.
[9] I. Ahmed, M. Sajed, A. Sultan, I. Murtaza, S. Yousaf, B. Maqsood, P. Vanhara, M. Anees, EXCLI J. 14 (2015) 916–925, http://dx.doi.org/10.17179/excli2015-207.
[10] S. Nastase, L. Bajenaru, C. Matei, R. Mitran, D. Berger, Micropor. Mesopor. Mater. 182 (2013) 32–39, http://dx.doi.org/10.1016/j.micromeso.2013.08.018.
[11] C. Lai, B. Trewyn, D. Jeftinija, K. Jeftinija, S. Xu, S. Jeftinija, V. Lin, J. Am. Chem. Soc. 125 (2003) 4451–4459, http://dx.doi.org/10.1021/ja028650l.
[12] A. Grumezescu, C. Ghitulica, G. Voicu, K.-S. Huang, C.-H. Yang, A. Ficai, B.S. Vasile, V. Grumezescu, C. Bleotu, M.C. Chifiriuc, Int. J. Pharm. 463 (2014) 170–176, http://dx.doi.org/10.1016/j.ijpharm.2013.07.016.
[13] A. Ramila, B. Munoz, P. Perez, V. Regi, J. Sol-Gel Sci. Technol. 26 (2003) 1199–1202, http://dx.doi.org/10.1023/A:1020764319963.
[14] C. Lin, S. Qiao, Z. Yu, S. Ismadji, G. Lu, Micropor. Mesopor. Mater. 117 (2009) 213–219, http://dx.doi.org/10.1016/j.micromeso.2008.06.023.
[15] F. Sevimli, A. Yılmaz, Micropor. Mesopor. Mater. 158 (2012) 281–291, http://dx.doi.org/10.1016/j.micromeso.2012.02.037.
[16] M. Seleem, P. Munusamy, A. Ranjan, H. Alqublan, G. Pickrell, Antimicrob. Agents Chemother. 53 (2009) 4270–4274, http://dx.doi.org/10.1128/AAC.00815-09.
[17] S. Hashemikia, N. Hemmatinejad, E. Ahmadi, M. Montazer, J. Colloid Interface Sci. 443 (2015) 105–114, http://dx.doi.org/10.1016/j.jcis.2014.11.020.
[18] I. Zahir, O. Sadeghi, R. Lotfizadeh, M. Amini, J. Sol-Gel Sci. Technol. 61 (2012) 90–95, http://dx.doi.org/10.1007/s10971-011-2595-4.
[19] M. Rosemary, I. MacLaren, T. Pradeep, Langmuir 22 (2006) 10125–10129.
[20] A. Maurya, P. Chauhan, A. Mishra, A. Pandey, J. Res. Updates Polym. Sci. 1 (2012) 43–51, http://dx.doi.org/10.6000/1929-5995.2012.01.01.6.
[21] M. Al Tameemi, D. Mihaiescu, R. Stan, A. Meghea, B. Vasile, V. Traistaru, D. Istrati, Dig. J. Nanomater. Biostruct. 10 (2015) 1229–1235. http://www.chalcogen.ro/1229_Tameemi.pdf.
[22] R. Lensing, A. Bleich, A. Smoczek, S. Glage, N. Ehlert, T. Luessenhop, P. Behrens, P.P. Müller, M. Kietzmann, M. Stieve, Acta Biomater. 9 (2013) 4815–4825, http://dx.doi.org/10.1016/j.actbio.2012.08.016.
[23] R. Yin, T. Agrawal, U. Khan, G. Gupta, V. Rai, Y. Huang, M. Hamblin, Nanomedicine (Lond.) 15 (2015) 2379–2404, http://dx.doi.org/10.2217/nnm.15.67.
[24] D. Stickler, Nat. Clin. Pract. Urol. 5 (2008) 598–608, http://dx.doi.org/10.1038/ncpuro1231.
[25] V. Prisacari, T. Ciaica, V. Tapcov, N. Samusi, Izonicotinoilhidrazona a aldehidei 5-nitro-2-furanice, Moldavian patent MD196 (1995).
[26] V. Prisacari, S. Buraciov, A. Dizdari, S. Stoleicov, V. Ţapcov, Communication I. Studies on Antibacterial Action, Scientific Annals

of the "N. Testemitanu" State University of Medicine and Pharmacy, Chisinau, 2002, pp. 255–259.
[27] V. Prisacari, S. Buraciov, A. Dizdari, S. Stoleicov, E. Diug, Scientific Annals of the "N. Testemitanu" State University of Medicine and Pharmacy, Chisinau I, 2003, pp. 240–243.
[28] J. McKinnell, N. Stollenwerk, C. Jung, L. Miller, Mayo Clin. Proc. 86 (2011) 480–488, http://dx.doi.org/10.4065/mcp.2010.0800.
[29] R. Spencer, D. Moseley, M. Greensmith, J. Antimicrob. Chemother. 33 (1994) 121–129, http://dx.doi.org/10.1093/jac/33.suppl_A.121.
[30] M. Al Tameemi, D. Gudovan, R. Stan, D. Mihaiescu, C. Ott, Rev. Rom. Mater. 43 (2014) 188–193. http://solacolu.chim.upb.ro/p188-193web.pdf.
[31] D. Mihaiescu, D. Tamas, E. Andronescu, A. Ficai, Dig. J. Nanomater. Biostruct. 9 (2014) 379–383. http://www.chalcogen.ro/379_Tamas.pdf.
[32] E. Stecoza, T. Căproiu, C. Drăghici, C. Chifiriuc, O. Drăcea, Rev. Chim. 60 (2009) 137–141. http://www.revistadechimie.ro/pdf/STECOZA%20CA.pdf.
[33] T. Rosu, S. Pasculescu, V. Lazar, C. Chifiriuc, R. Cernat, Molecules 11 (2006) 904–914, http://dx.doi.org/10.3390/11110904.
[34] C. Limban, M. Balotescu, A. Missir, I. Chiriță, C. Bleotu, Molecules 13 (2008) 567–580, http://dx.doi.org/10.3390/molecules13030567.
[35] A. Grumezescu, E. Andronescu, A. Ficai, C. Bleotu, D. Mihaiescu, M. Chifiriuc, Int. J. Pharm. 436 (2012) 771–777, http://dx.doi.org/10.1016/j.ijpharm.2012.07.063.
[36] C. Chifiriuc, V. Grumezescu, M. Grumezescu, M. Saviuc, V. Lazar, E. Andronescu, Nanoscale Res. Lett. 7 (2012) 209, http://dx.doi.org/10.1186/1556-276X-7-209.
[37] H. Dewen, B. Cancheng, J. Chongwen, Z. Tao, Powder Technol. 249 (2013) 151–156, http://dx.doi.org/10.1016/j.powtec.2013.07.026.
[38] R. Mueller, H.K. Kammler, K. Wegner, S.E. Pratsinis, Langmuir 19 (2003) 160–165.
[39] M. Schmidt, K. Baldridge, J. Boatz, S. Elbert, M. Gordon, J. Jensen, S. Koseki, N. Matsunaga, K. Nguyen, S. Su, T. Windus, M. Dupuis, J. Montgomery, J. Comput. Chem. 14 (1993) 1347–1363, http://dx.doi.org/10.1002/jcc.540141112.
[40] M. Bode, S. Gordon, J. Mol. Graph. Model. 16 (1998) 133–138, http://dx.doi.org/10.1016/S1093-3263(99)00002-9.
[41] A. Allouche, J. Comput. Chem. 32 (2011) 174–182, http://dx.doi.org/10.1002/jcc.21600.
[42] D. Guay, Drugs 61 (2001) 353–364, http://dx.doi.org/10.2165/00003495-200161030-00004.
[43] G. Timmins, V. Deretic, Mol. Microbiol. 62 (2006) 1220–1227, http://dx.doi.org/10.1111/j.1365-2958.2006.05467.